metals

MDPI

Article

Upgrading of High-Aluminum Hematite-Limonite Ore by High Temperature Reduction-Wet Magnetic Separation Process

Xianlin Zhou *, Deqing Zhu, Jian Pan, Yanhong Luo and Xinqi Liu

School of Mineral Processing and Bioengineering, Central South University, Changsha 410083, China; dqzhu@csu.edu.cn (D.Z.); pjcsu@csu.edu.cn (J.P.); yhluo_csu@163.com (Y.L.); lxqcoolsir@csu.edu.cn (X.L.)
* Correspondence: xlzhou_csu@csu.edu.cn; Tel./Fax: +86-731-8883-6942

Academic Editor: Hugo F. Lopez
Received: 8 January 2016; Accepted: 3 March 2016; Published: 8 March 2016

Abstract: The huge consumption of iron ores in China has attracted much attention to utilizing low grade complex iron resources, such as high-aluminum hematite-limonite ore, which is a refractory resource and difficult to upgrade by traditional physical concentration processes due to the superfine size and close dissemination of iron minerals with gangue minerals. An innovative technology for a high temperature reduction-magnetic separation process was studied to upgrade a high-aluminum iron ore assaying 41.92% Fe_{total}, 13.74% Al_2O_3 and 13.96% SiO_2. The optimized results show that the final metal iron powder, assaying 90.46% Fe_{total}, was manufactured at an overall iron recovery of 90.25% under conditions as follows: balling the high aluminum iron ore with 15% coal blended and at 0.3 basicity, reducing the dried pellets at 1350 °C for 25 min with a total C/Fe mass ratio of 1.0, grinding the reduced pellets up to 95%, passing at 0.074 mm and magnetically separating the ground product in a Davis Tube at a 0.10-T magnetic field intensity. The metal iron powder can be used as the burden for an electric arc furnace (EAF). Meanwhile, the nonmagnetic tailing is suitable to produce ceramic, which mainly consists of anorthite and corundum. An efficient way has been found to utilize high-aluminum iron resources.

Keywords: high-aluminum hematite-limonite ore; aluminum-iron separation; high temperature reduction; wet magnetic separation

1. Introduction

The growth of the Chinese iron steel industry has been pushed forward by its rapid economic development in recent years, and 1126 million tons of iron ore have been consumed in 2014, where 933 million tons were imported according to the data from Worldsteel Association [1]. However, iron resources are limited, and the reserves of high-grade iron ores are declining, so it is of great importance to optimize the mining rate of iron resources [2] and to utilize low-grade refractory iron resources, such as high-aluminum limonite ores.

High-aluminum limonite ore is a typical refractory resource; it is difficult to upgrade by traditional processes due to the superfine size and close dissemination of iron minerals with gangue minerals [3,4]. Some high-aluminum iron ores were directly blended in a sintering mixture at a low ratio, but the sintering process and the properties of the product sinter were adversely affected, which was reviewed by Lu *et al.* [5]. Meanwhile, high-aluminum ore affects the viscosity and desulfurizing capacity of blast furnace slag [6]. Many upgrading approaches have been published for high-aluminum limonite ore, including physical and chemical processes [4]. Recent research was focused on gravity concentration and magnetic separation [7], flotation [8,9], sodium roasting and the magnetic separation process [3,10–15]. However, iron and aluminum cannot be separated completely by physical processes,

so iron recovery is low by the flotation process (around 70%), and as high as beyond 10% of sodium additive is needed by the sodium roasting process, which brings the risk of the degradation of refractory materials in furnaces [16,17] and higher costs.

The coal-based direct reduction-magnetic separation process is an efficient way to recover iron from low-grade complex iron ores [18] and secondary resources containing ferrous material, such as copper slag [19]. However, a low reduction rate is a problem of the reduction process, which is always operated under 1100–1200 °C for more than 60 min. Elevating the reduction temperature is an effective means to promote the reduction rate of iron minerals. Therefore, a novel technology of high temperature reduction-wet magnetic separation of high-aluminum limonite is studied in this paper.

2. Materials and Methods

2.1. Raw Materials

The chemical compositions of high-aluminum hematite-limonite ore used in this study are tabulated in Table 1. The total iron grade of the ore sample is 41.92%, and high alumina and silica contents were observed, assaying 13.74% Al_2O_3 and 13.96% SiO_2, respectively. Combining with the X-ray diffraction (XRD) results shown in Figure 1, iron minerals mainly consist of hematite and goethite, and the aluminum mineral is kaolinite. Figures 2 and 3 illustrate representative SEM-EDS and optical micrographs of ore samples, which indicate that hematite is closely included with kaolinite, leading to significant difficulties in the separation of iron and aluminum.

Table 1. Chemical compositions of high-aluminum hematite-limonite ore (wt. %).

Chemical Compositions (wt. %)													
Fe_{total}	FeO	Al_2O_3	SiO_2	CaO	MgO	Mn	K_2O	Na_2O	P	S	Pb	Zn	LOI
41.92	0.17	13.74	13.96	0.13	0.88	1.24	0.42	0.03	0.13	0.01	0.64	0.21	7.20

Note: LOI, loss on ignition.

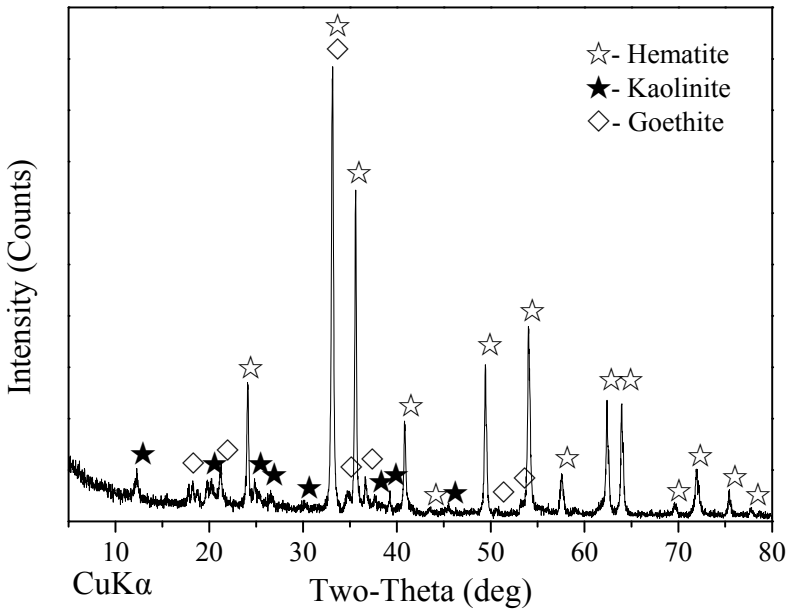

Figure 1. XRD pattern of high-aluminum hematite-limonite ore.

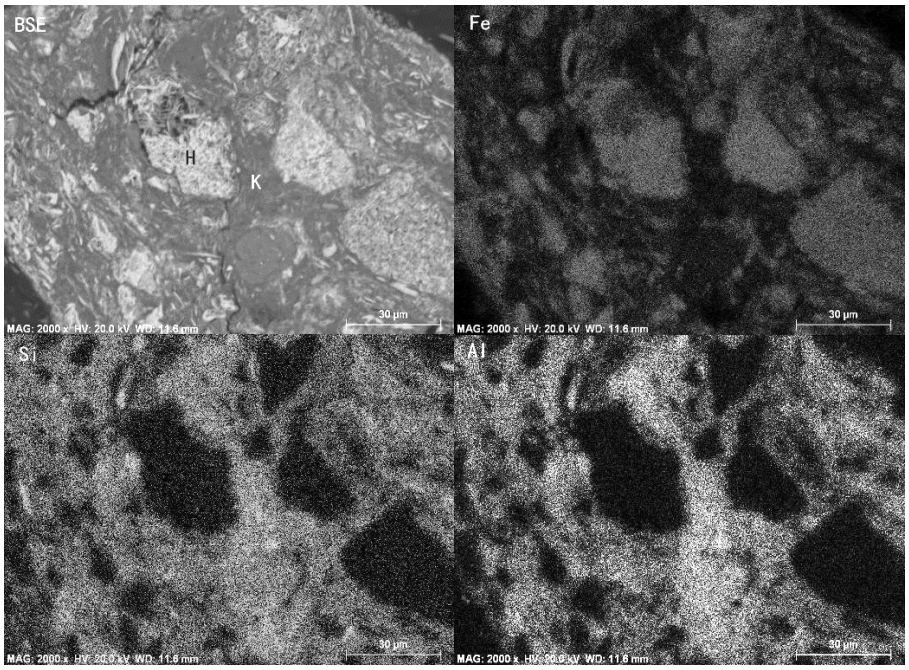

Figure 2. Representative SEM-BSE micrographs of high-aluminum hematite-limonite ore. (BSE, Back Scattered Electron Imaging; H, hematite; K, kaolinite).

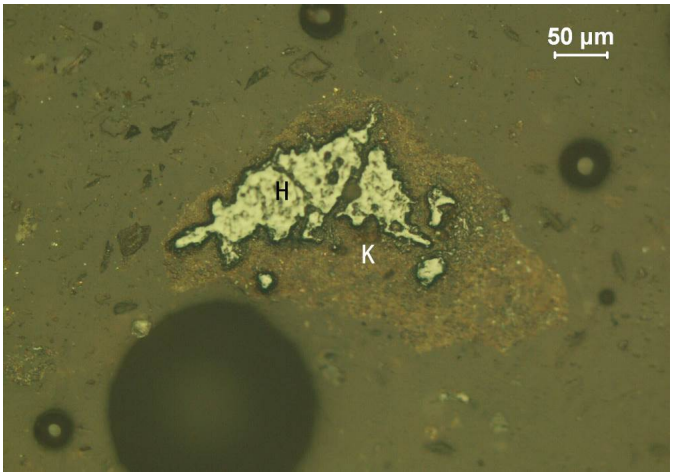

Figure 3. Granular hematite (H) filled in the particles of kaolinite (K) under reflected light.

$CaCO_3$ of analytical grade was used to adjust the binary basicity of blends.

The soft coal was used as a reductant agent, with fixed carbon of 52.12% on an air dry basis (FCad), volatile matter of 30.41% on a dry ash free (Vdaf) basis, ash of 4.49% on an air dry basis (Aad), 0.58% of S and a melting temperature of 1376 °C. Coal ash possesses high silica, calcium oxide and sulfur content, as listed in Table 2. Soft coal as a reductant is 100% passing at 5 mm, and some soft coal used for blending in the pellet feed was milled to 100% passing at 0.074 mm.

Table 2. Chemical compositions of coal ash (wt. %).

Chemical Compositions (wt. %)									
Fe_{total}	Fe_2O_3	SiO_2	Al_2O_3	CaO	MgO	K_2O	Na_2O	P	S
11.80	16.70	27.62	8.02	24.94	1.34	0.16	1.34	0.01	12.92

2.2. Experimental Procedures

The experimental flow sheet includes procedures as follows: mixing the ore with $CaCO_3$ and soft coal, pelletizing of the mixture, high temperature reduction roasting of dried pellets, grinding the reduced pellets and low intensity magnetic separation of the ground product to manufacture metal iron powder.

Mixtures were prepared by mixing the ore, $CaCO_3$ and soft coal fines. The mass of $CaCO_3$ was determined by binary basicity, and the soft coal mass blended in pellets was calculated by the coal-bearing mass ratio multiplied by the mass of the iron ore sample. Then, green balls were made by balling the mixtures in a disc pelletizer of 0.8 m in diameter and a 0.2 m rim depth, rotating at 38 rpm and being inclined at 47° to the horizontal. The screened green balls of 8–16 mm were loaded into the drying oven to dry at 105 °C for 2 h until the weight was unchanged.

The dried pellets were put into the corundum crucible and covered by some soft coal, where the mass of soft coal was determined by the C/Fe mass ratio. The crucible was covered by a graphite cover and put into the muffle furnace (model: KSY-12-18, The Great Wall Furnace, Changsha, China), while the reducing temperature was elevated to the target value. When the reduction time was ended, the hot crucible was taken out and covered by pulverized coal to cool down quickly in the air to prevent the reduced pellets from being re-oxidized.

The magnetic separation was performed in the Davis Tube (model: XCGS-73, Changsha Research Institute of Mining and Metallurgy Co., Changsha, China) after 20 g of reduced pellets were ground in the cone ball mill (model: RK/ZQMØ160×60, Wuhan Rock Crush & Grand Equipment Manufacture Co., Wuhan, China). The metal iron powder was obtained after magnetic separation. The grinding fineness of reduced pellets was about 95% passing at 0.074 mm, and the magnetic field intensity was 0.10 T.

The chemical compositions of the ore and metal iron powder were measured by X-ray fluorescence spectroscopy (XRF, PANalytical Axios mAX, PANalytical B.V., Almelo, The Netherlands). The crystalline phase composition of the material was determined using an X-ray diffractometer (XRD, D/Max-2500, Rigaku Co., Tokyo, Japan). Proximate analysis of coal and the determination of the fusibility of coal ash were conducted by the Chinese standards GB/T212-2008 and GB/T219-2008, respectively. Microstructures of reduced pellets were observed by scanning electron microscope (SEM, FEI Quanta-200, FEI Company, GG Eindhoven, The Netherlands), and the compositional analyses were carried out using an energy dispersion system (EDAX-TSL, Ametek Inc., Paoli, CO, USA) within the SEM.

2.3. Thermodynamic Analysis of Reduction Process

Equations (1)–(18) show the possible reactions during the reduction process of high-aluminum hematite-limonite ore, and FactSage7.0 (Thermfact/CRCT, Montreal, QC, Canada; GTT-Technologies, Herzogenrath, Germany) is applied to calculate the Gibbs energy changes of all of the reactions; the results are depicted in Figures 4 and 5. In Figure 4, the line of Equation (1) is intersected by the lines of Equation (3) and Equation (4) at T_1 and T_2. Because of the Boudouard reaction (Equation (1)), the CO concentration is higher than that of Equations (2)–(4) at a temperature over T_2, so the metallic iron begins to appear (Equation (4)) where the CO concentration is over 58%. During T_1 to T_2, Fe_3O_4 is reduced to FeO (Equation (3)), and the CO concentration is between 42% and 58%. The region of $T_1 < T < T_2$ is the stable zone of the FeO phase. When the temperature is lower than T_1, the CO concentration is still higher than that of Equation (2), so Fe_2O_3 is reduced to Fe_3O_4 (Equation (2)). Consequently, the regions of $T < T_1$, $T_1 < T < T_2$ and $T > T_2$ are the equilibrium stable fields of Fe_3O_4, FeO and Fe, respectively. Theoretically, the reduction of iron oxide by solid carbon follows the steps as $Fe_2O_3 \rightarrow Fe_3O_4 \rightarrow FeO \rightarrow Fe$ beyond T_2; transformations $Fe_2O_3 \rightarrow Fe_3O_4$ and $Fe \rightarrow FeO \rightarrow Fe_3O_4$ will occur when the reduction temperature is lower than T_1; while $Fe_2O_3 \rightarrow Fe_3O_4 \rightarrow FeO$ and $Fe \rightarrow FeO$ are the steps between T_1 and T_2 [20]. It is demonstrated that iron oxide is reduced by stepwise deoxidation, and wüstite (FeO) is an intermediate product. Because of the presences of SiO_2 and Al_2O_3,

wüstite can easily chemically combine with them to form fayalite (Fe_2SiO_4; refer to Equation (6)) and hercynite ($FeAl_2O_4$; refer to Equation (7)). Meanwhile, mullite ($Al_6Si_2O_{13}$) may occur by the reaction between SiO_2 and Al_2O_3 (Equation (8)) and then is degraded by FeO to form fayalite and hercynite (Equations (9) and (10)), both of which are unable to be reduced by CO thermodynamically [19,21]. Thus, solid carbon is used as the reductant, where fayalite and hercynite can be reduced beyond 805 and 830 °C, respectively. Moreover, alkaline-earth oxide can improve the reduction of fayalite and hercynite by reacting with SiO_2 and Al_2O_3 chemically to form larnite (Ca_2SiO_4) and calcium aluminate ($CaAl_2O_4$), respectively.

$$C + CO_2 = 2CO \quad (1)$$

$$3Fe_2O_3 + CO = 2Fe_3O_4 + CO_2\, T > 570\,^{\circ}C \quad (2)$$

$$Fe_3O_4 + CO = 3FeO + CO_2\, T > 570\,^{\circ}C \quad (3)$$

$$FeO + CO = Fe + CO_2\, T > 570\,^{\circ}C \quad (4)$$

$$1/4Fe_3O_4 + CO = 3/4Fe + CO_2\, T < 570\,^{\circ}C \quad (5)$$

$$2FeO + SiO_2 = Fe_2SiO_4 \quad (6)$$

$$FeO + Al_2O_3 = FeAl_2O_4 \quad (7)$$

$$3Al_2O_3 + 2SiO_2 = Al_6Si_2O_{13} \quad (8)$$

$$4FeO + Al_6Si_2O_{13} = 2Fe_2SiO_4 + 3Al_2O_3 \quad (9)$$

$$3FeO + Al_6Si_2O_{13} = 3FeAl_2O_4 + 2SiO_2 \quad (10)$$

$$Fe_2SiO_4 + 2CO = 2Fe + SiO_2 + 2CO_2 \quad (11)$$

$$FeAl_2O_4 + CO = Fe + Al_2O_3 + CO_2 \quad (12)$$

$$Fe_2SiO_4 + 2C = 2Fe + SiO_2 + 2CO \quad (13)$$

$$FeAl_2O_4 + C = Fe + Al_2O_3 + CO \quad (14)$$

$$Fe_2SiO_4 + 2CaO + 2CO = 2Fe + Ca_2SiO_4 + 2CO_2 \quad (15)$$

$$FeAl_2O_4 + CaO + CO = Fe + CaAl_2O_4 + CO_2 \quad (16)$$

$$Fe_2SiO_4 + 2CaO + 2C = 2Fe + Ca_2SiO_4 + 2CO \quad (17)$$

$$FeAl_2O_4 + CaO + C = Fe + CaAl_2O_4 + CO \quad (18)$$

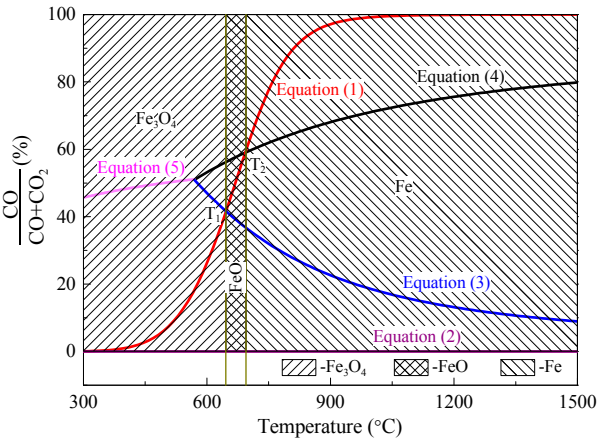

Figure 4. Gas-phase equilibrium of iron oxides reduced by solid carbon.

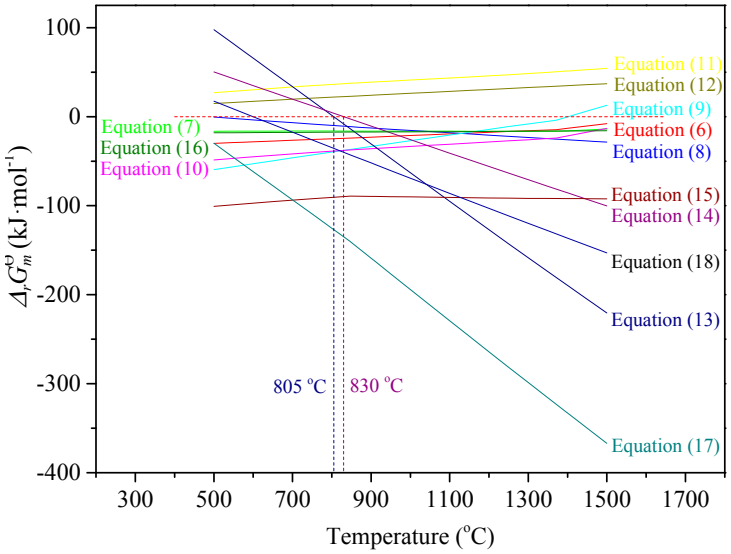

Figure 5. Calculations of Gibbs energy changes of Equations (6)–(18) by FactSage7.0.

It can be illustrated that it is difficult to separate aluminum and silica with iron by reducing the high-aluminum hematite-limonite ore only under a CO atmosphere; solid carbon and alkaline-earth oxide should be blended to enhance the reduction process to improve the separation of iron with impurities.

3. Results and Discussion

3.1. Dosage of Reductant

The effect of reductant dosage on the reduction and separation processes is shown in Figure 6. It shows that the optimum metallization degree, iron grade and recovery were achieved at 1.0 of the carbon to iron (C/Fe) mass ratio, where the iron grade is 90.58%. However, only part of the iron was reduced to metallic iron; both the metallization degree and iron recovery were lower than 60%.

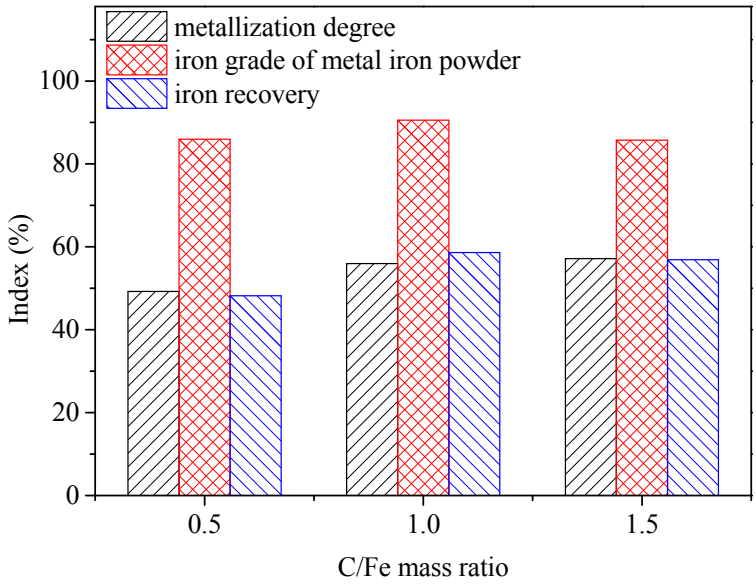

Figure 6. Effect of C/Fe mass ratio on the reduction and separation indexes (reducing at 1300 °C for 20 min).

The coal-bearing process is an efficient means to enhance the reduction of complex iron ore because the process can be self-sufficient chemically to complete the task of metallization if the required heat is supplied [22,23]. Based on thermodynamic analysis, different coal-bearing mass ratios were investigated to reveal the effects of coal-bearing ratio on the reduction and separation process, where the coal-bearing mass ratio was defined as the division of the masses between the bearing coal and iron ore. Results in Figure 7 show that the metallization degree of reduced pellets is elevated dramatically by coal-bearing mass ratio increases from 0%–15%, and iron recovery is over 90% when the ratio is 15%. However, the iron grade of metal iron powder after magnetic separation is on a downward trend when the ratio is beyond 15% because of the high impurity contents in coal ash.

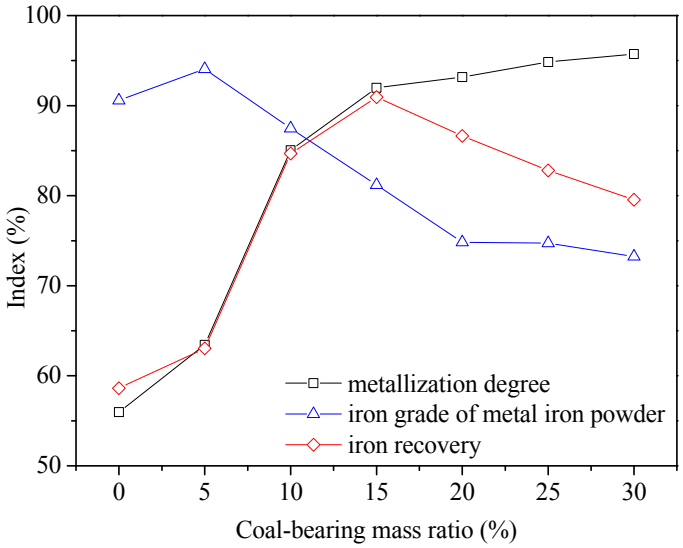

Figure 7. Effect of coal-bearing mass ratio on the reduction and separation indexes (reducing at 1300 °C for 20 min with a total C/Fe mass ratio of 1.0).

Fayalite and hercynite are detected in the reduced pellets of blends without coal-bearing, as illustrated in Figure 8, leading to a lower metallization degree and iron recovery. Due to the low melting temperature of fayalite, the liquid phase formed easily in the reduction temperature range, and micromelting appearance was observed in the reduced pellets. Distributions of iron grains in Figure 9 demonstrate that metallic iron grains exist at the outer layer of reduced pellets without coal-bearing, and the inner layer is filled with fayalite and hercynite. In contrast, dominant iron minerals are reduced to metallic iron at both the inner and outer layer by blending 15% coal fines in the pellet feed, and minor iron minerals combine with Al_2O_3 to form a trace of hercynite. Mullite is the main gangue mineral, which inhibits the grain growth of metal iron to a certain extent, so that there are still some metallic iron grains with fine particle size less than 20 μm, resulting in the low iron grade of the metal iron powder after magnetic separation.

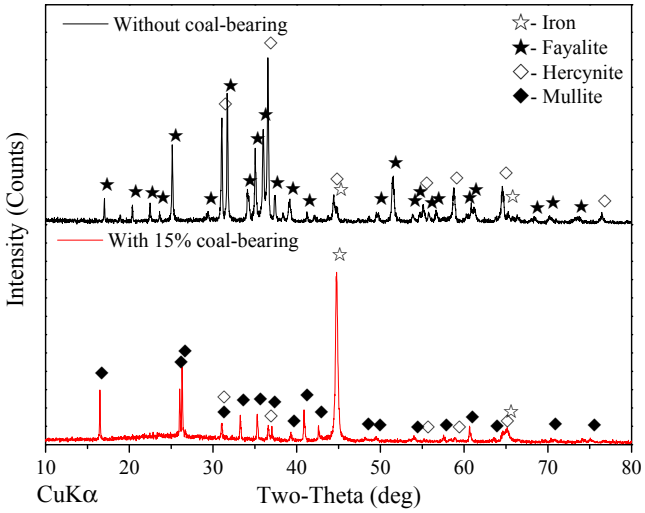

Figure 8. XRD patterns of reduced pellets with different coal-bearing mass ratios (reducing at 1300 °C for 20 min with a total C/Fe mass ratio of 1.0).

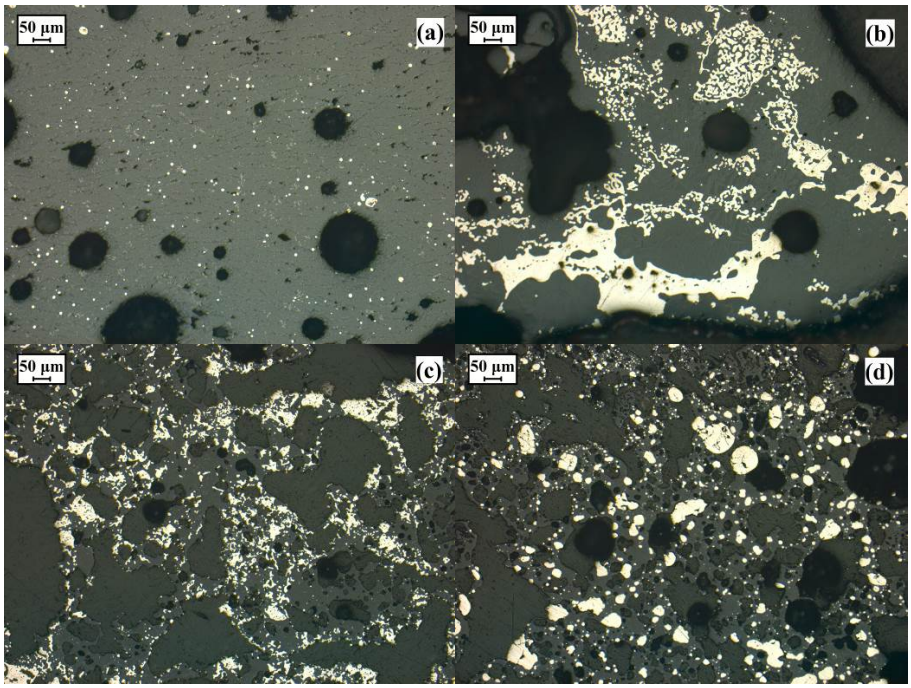

Figure 9. Distributions of iron grains in reduced pellets under different coal-bearing mass ratios ((**a**,**b**) inner and outer layer without coal-bearing; (**c**,**d**) inner and outer layer with a 15% coal-bearing mass ratio).

3.2. Optimization of Reduction Parameters

The iron grade of metal iron powder was raised from 81.83%–91.05% by increasing the reduction temperature from 1250–1400 °C, as demonstrated in Figure 10. The reduction temperature is an important factor that affects the reaction kinetics; a higher reduction temperature can promote the migration and growth rate of metal iron grains during the reduction process. By considering economic efficiency, the reduction temperature was suggested to be 1350 °C for further research.

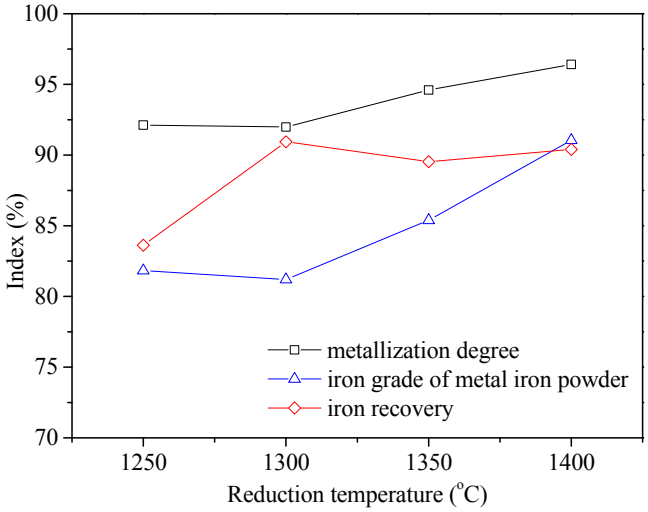

Figure 10. Effect of the reduction temperature on the reduction and separation indexes (reducing for 20 min with a total C/Fe mass ratio of 1.0, 15% coal blended in pellets).

Figure 11 presents the effect of reduction duration on the indexes of the reduction and separation processes, which shows that the metallization degree and iron recovery were enhanced by prolonging the reduction duration from 20–25 min. Further extension of the reduction time had a slightly negative impact on the indexes. Therefore, reducing at 1350 °C for 25 min was recommended, where the metal iron powder was manufactured with 85.00% of iron grade at a recovery of 92.05%, respectively.

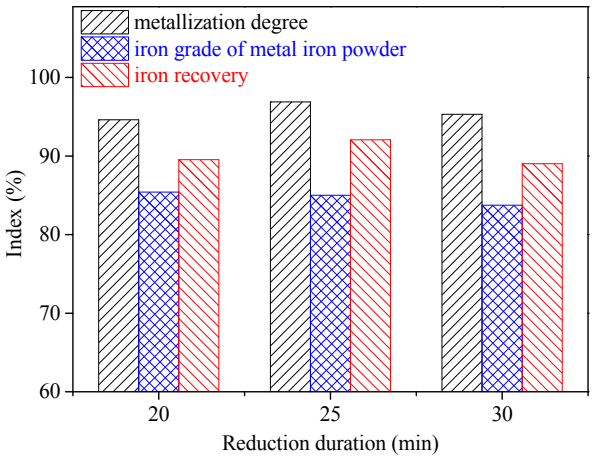

Figure 11. Effect of reduction duration on the reduction and separation indexes (reducing at 1350 °C with a total C/Fe mass ratio of 1.0, 15% coal blended in pellets).

3.3. Effect of Binary Basicity

The effects of binary basicity (ratio of CaO/SiO_2) on the reduction and separation process are shown in Figure 12. The metallization degree of reduced pellets increases slightly and then keeps steady when basicity is elevated from 0.02 (natural basicity) to 0.5; the beneficiation of iron concentrate is improved, where the iron grade keeps increasing from 85.00%–92.64% while the recovery of iron is over 90%. XRD of the reduced pellets with 0.3 basicity in Figure 13 proves that most iron minerals are reduced to metallic iron; impurities, such as alumina and silica, react with calcium oxide to form anorthite ($CaAl_2Si_2O_8$); and the rest of the alumina exists as corundum. Metallic iron grains migrated and agglomerated together to generate coarser particles (refer to Figure 14), contributing to higher

iron grade and recovery in magnetic separation because of the higher liberation degree of the metal iron grains in grinding.

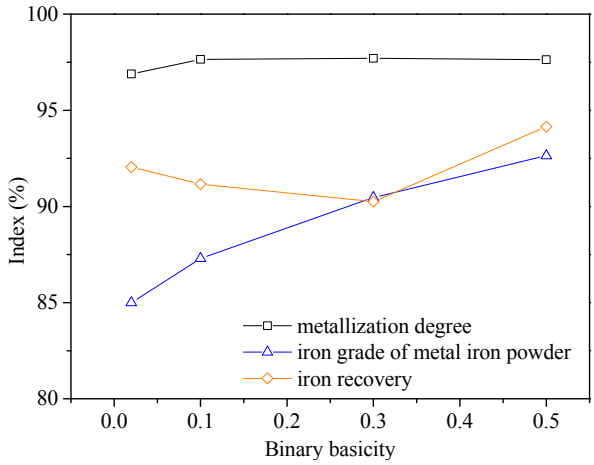

Figure 12. Effect of binary basicity on the reduction and separation indexes (reducing at 1350 °C for 25 min with a total C/Fe mass ratio of 1.0, 15% coal blended in pellets).

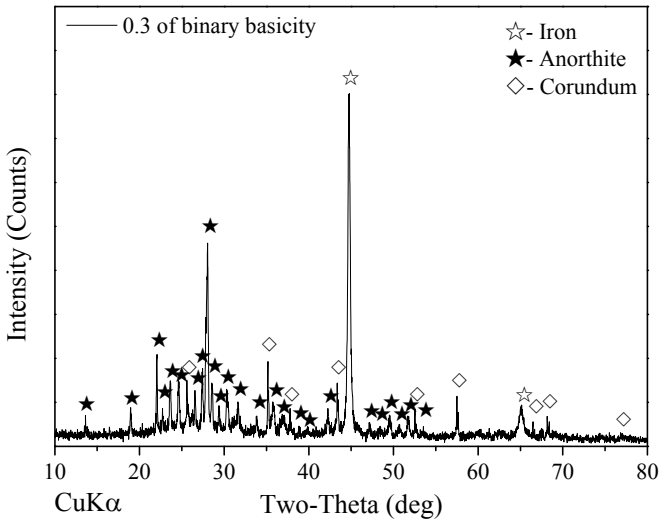

Figure 13. Main minerals in reduced pellets with a binary basicity of 0.3 detected by XRD.

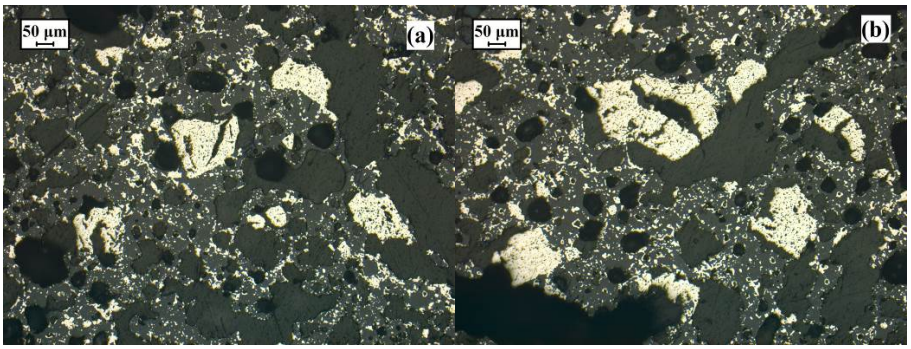

Figure 14. Distributions of metallic iron grains in reduced pellets at 0.3 binary basicity ((**a**,**b**) inner and outer layer, reducing at 1350 °C for 25 min with a total C/Fe mass ratio of 1.0).

In summary, the optimum conditions were recommended as follows: preparing the green balls by blending 15% coal and $CaCO_3$ at 0.3 basicity with iron ore, reducing the dried pellets at 1350 °C for 20 min with a total C/Fe mass ratio of 1.0 and magnetic separating of the ground reduced pellets with a size up to 95% passing at 0.074 mm and at a 0.10-T magnetic field intensity. Table 3 presents the chemical compositions of final products. The metal iron powder assaying 90.46% Fe_{total} was achieved at an overall iron recovery of 90.25%. The final product can be applied as the burden for an electric arc furnace, and the nonmagnetic tailings can be used to produce ceramic and glass [24,25]; the green utilization of high-aluminum iron resources is probably achieved.

Table 3. Chemical compositions of final products (wt. %).

Sample	Fe_{total}	Al_2O_3	SiO_2	CaO	MgO	MnO	K_2O	Na_2O	P	S
Metal iron powder	90.46	4.57	3.57	0.48	0.23	0.42	0.09	0.04	0.025	0.007
Nonmagnetic tailings	9.97	34.64	37.99	8.63	1.71	2.81	1.64	0.27	0.040	0.101

4. Conclusions

(1) A high-aluminum hematite-limonite ore, assaying 41.92% Fe_{total}, 13.74% Al_2O_3 and 13.96% SiO_2, was used as the raw material to manufacture metal iron powder, where iron minerals mainly occur in hematite and goethite and aluminum minerals exist in kaolinite. Hematite is closely disseminated with kaolinite, leading to harder separation between iron and alumina.

(2) Good quality metal iron powder assaying 90.46% Fe_{total} was produced at an overall iron recovery of 90.25% under the following conditions: balling the mixture of iron ore with 15% coal and $CaCO_3$ fines at 0.3 basicity, reducing the dried pellets at 1350 °C for 25 min and with a total C/Fe mass ratio of 1.0, grinding the reduced pellets up to 95% passing at 0.074 mm and magnetic separation in a Davis Tube at 0.10 T of magnetic field intensity.

(3) The process provides a potential way to utilize high-aluminum iron ore, where the good quality metal iron powder can be used as the burden for EAF and nonmagnetic tailings can be applied in ceramic and glass industries.

Acknowledgments: This work was financially supported by the Co-Innovation Center for Clean and Efficient Utilization of Strategic Metal Mineral Resources and the National Key Technology R&D Program of China (No. 2013BAB03B04).

Author Contributions: Xianlin Zhou and Deqing Zhu conceived of and designed the experiments. Xianlin Zhou, Yanhong Luo and Xinqi Liu performed the experiments. Xianlin Zhou and Jian Pan analyzed the data. Deqing Zhu and Jian Pan contributed materials. Xianlin Zhou wrote the paper.

Conflicts of Interest: The authors declare no conflict of interest.

References

1. *Steel Statistical Yearbook 2015*; World Steel Association: Brussels, Belgium, 2015; p. 105.
2. Zhang, K.; Kleit, A.N. Mining rate optimization considering the stockpiling: A theoretical economics and real option model. *Resour. Policy* **2016**, *47*, 87–94. [CrossRef]
3. Jiang, T.; Liu, M.; Li, G.; Sun, N.; Zeng, J.; Qiu, G. Novel process for treatment of high-aluminum limonite ore by reduction roasting with addition of sodium salts. *Chin. J. Nonferr. Met.* **2010**, *20*, 565–571.
4. Shu, C.; Tang, Y.; Wang, Z.; Zhang, Q. Research on sodium salt roasting-acid leaching technology for high-alumina and high-silicon refractory limonite. *Min. Metall. Eng.* **2012**, *32*, 62–65.
5. Lu, L.; Holmes, R.J.; Manuel, J.R. Effects of alumina on sintering performance of hematite iron ores. *ISIJ Int.* **2007**, *47*, 349–358. [CrossRef]
6. Tian, Q.; Shi, Y. Research on desulfurizing capacity of high Al_2O_3 content slag. *Ironmaking* **1998**, *17*, 32–33.
7. Raghukumar, C.; Tripathy, S.K.; Mohanan, S. Beneficiation of Indian high alumina iron ore fines—A case study. *Int. J. Min. Eng. Miner. Process.* **2012**, *1*, 94–100. [CrossRef]

8. Thella, J.S.; Mukherjee, A.K.; Srikakulapu, N.G. Processing of high alumina iron ore slimes using classification and flotation. *Powder Technol.* **2012**, *217*, 418–426. [CrossRef]
9. Jain, V.; Rai, B.; Waghmare, U.V.; Tammishetti, V. Pradip Processing of Alumina-Rich Iron Ore Slimes: Is the Selective Dispersion-Flocculation-Flotation the Solution We Are Looking for the Challenging Problem Facing the Indian Iron and Steel Industry? *Trans. Indian Inst. Met.* **2013**, *66*, 447–456. [CrossRef]
10. Chun, T.J.; Zhu, D.Q.; Pan, J.; He, Z. Preparation of metallic iron powder from red mud by sodium salt roasting and magnetic separation. *Can. Metall. Quart.* **2014**, *53*, 183–189. [CrossRef]
11. Li, G.; Zhou, T.; Liu, M.; Jiang, T.; Fan, X. Novel process and mechanisms of aluminum-iron separation of high-aluminum limonite ore. *Chin. J. Nonferr. Met.* **2008**, *18*, 2087–2093.
12. Li, G.; Liu, M.; Jiang, T.; Zhou, T.; Fan, X. Mineralogy charateristics and separation of aluminum and iron of high-aluminum iron ores. *J. Cent. South Univ.* **2009**, *18*, 1165–1171.
13. Jiang, T.; Liu, M.; Li, G.; Sun, N.; Zeng, J.; Qiu, G. Effects of sodium-salt on Al-Fe separation by reduction roasting for high-aluminum content limonite. *Chin. J. Nonferr. Met.* **2010**, *20*, 1226–1233.
14. Li, G.; Jiang, T.; Liu, M.; Zhou, T.; Fan, X.; Qiu, G. Beneficiation of high-aluminium-content hematite ore by soda ash roasting. *Min. Proc. Ext. Met. Rev.* **2010**, *31*, 150–164. [CrossRef]
15. Chun, T.; Long, H.; Li, J. Alumina-iron separation of high alumina iron ore by carbothermic reduction and magnetic separation. *Sep. Sci. Technol.* **2015**, *50*, 760–766. [CrossRef]
16. Stjernberg, J.; Olivas-Ogaz, M.A.; Antti, M.L.; Ion, J.C.; Lindblom, B. Laboratory scale study of the degradation of mullite/corundum refractories by reaction with alkali-doped deposit materials. *Ceram. Int.* **2013**, *39*, 791–800. [CrossRef]
17. Stjernberg, J.; Antti, M.; Nordin, L.; Odén, M. Degradation of refractory bricks used as thermal insulation in rotary kilns for iron ore pellet production. *Int. J. Appl. Ceram. Technol.* **2009**, *6*, 717–726. [CrossRef]
18. Zhu, D.; Zhou, X.; Pan, J.; Luo, Y. Direct reduction and beneficiation of a refractory siderite lump. *Miner. Process. Extr. Metall.* **2014**, *123*, 246–250. [CrossRef]
19. Zhou, X.; Zhu, D.; Pan, J.; Wu, T. Utilization of waste copper slag to produce directly reduced iron for weathering resistant steel. *ISIJ Int.* **2015**, *55*, 1347–1352.
20. Huang, X. *Ferrous Metallurgy Theory*, 4th ed.; Metallurgical Industry Press: Beijing, China, 2005; pp. 413–437.
21. Zhang, B.; Wang, Z.; Gong, X.; Guo, Z. Study on reduction of high-aluminum iron ores with gas in a fluidized bed (in Chinese). *J. Chin. Soc. Rare Earth.* **2013**, *30*, 774–780.
22. Wei, Y.; Sun, T.; Kou, J.; Yu, W.; Cao, Y. Effect of coal dosage on direct reduction roasting of refractory iron ore briquettes. *J. Cent. South Univ.* **2013**, *44*, 1305–1311.
23. Lu, W.; Huang, D.F. The evolution of ironmaking process based on coal-containing iron ore agglomerates. *ISIJ Int.* **2001**, *41*, 807–812. [CrossRef]
24. Gu, X.; Dong, W.; Chen, Y.; Li, Y. Investigation on the glass-anorthite insulating composites with low dielectric constant and low sintering temperature. *Rare Metal Mater. Eng.* **2007**, *36*, 464–467.
25. Liu, Q.; Pan, Z.; Li, Q.; Ruan, Y. Preparation of anorthite lightweight thermal insulating brick and the formation process of anorthite. *Bull. Chin. Ceram. Soc.* **2010**, *29*, 1269–1274.